High signal-to-noise ratio LDV measurements of pipe flow at low-moderate Reynolds number

F. Esposito[1], E. Nino[2] and C. Serio[1]

[1]Gruppo Collegato di Potenza, Sezione INFM di Napoli,
C.da Macchia Romana, 85100 Potenza
[2]Dipartimento di Ingegneria e Fisica dell'Ambiente,
Università della Basilicata, Potenza, Italy

May 19, 2000

ABSTRACT

Low Reynolds number velocity flow has been investigated in a horizontal cylindrical duct (internal diameter=0.05 m and length = 6.00 m) by a custom made Laser Doppler Velocimetry system. The LDV facility was based on a 20 mW HeNe laser, some manipulation optics and a novel electro-optic phase modulator for frequency shifting. Because of the low Reynolds number investigated, the noise introduced into the signal by commercial frequency shifters (e.g. Bragg cells) was not acceptable. The new device we have developed is based on a commercially available electro-optic crystal (Pockels cell) constituted by four potassium dihydrogen phosphate KDP (KD2PO4) of aperture of 3*3 mm. The LDV system has been used to analyse the power spectrum of the velocity fluctuations. An exponential falls off of the spectrum with frequency has been clearly evidenced.

1.Introduction

Scaling laws which cannot be deduced by simple dimensional arguments are generally referred to as being anomalous (e.g. [1]). Anomalous scaling arises in physical systems which are not linear and whose properties are better described in terms of fractal geometry (e.g. [2]). Fluid turbulence is perhaps the most celebrated example of physical phenomenon showing anomalous scaling. Since the measurements by Anselmet et al [3], who experimentally evidenced anomalous scaling at inertial range scales, it has been a common conception that non-linearity is peculiar to the inertial range, where inertia effects dominate over viscosity. Recently, Benzi et al [4, 5] have evidenced that this is a misconception. Non-linear effects are important even in the dissipative (viscous) range and a new kind of relative scaling among the structure functions themselves may be defined which extends from the smallest resolvable scales to the integral scale of turbulence [4, 5]. Benzi et al [4, 5] termed this new form of scaling Extended Self-Similarity (ESS) and provided both numerical and experimental evidence for its validity.

Evidence of ESS scaling for very low Reynolds number has been recently provided by Esposito et al [6] who examined pipe flow. Measurements at very low Reynolds numbers are quite useful in the aim of ESS, since for these Re values the dissipative range can be easily evidenced with state-of-art velocity probes. Quite recently, evidence of ESS has been also established for grid turbulence in the regime of very low Reynolds number [7]. Further evidence for ESS scaling in the range of low Reynolds number have been provided by one of the author [8] who showed that the probability density function of the velocity increments has the stretched exponential form. A result which perfectly parallels that already known for fully developed turbulence (e.g., [9]). It has been suggested that the most singular events generate anomalous scaling which intimately links this form of scaling to intermittency. Kraichnan [10] showed that an intermittent behaviour has to characterize the flow provided that the spectrum falls-off faster than algebraically.

In this paper, direct experimental evidence of stronger than algebraic fall-off of the variance spectrum at very low Reynolds number is provided. It has to be stressed that Kraichnan's arguments [10] are independent of Reynolds number (Re) so that our findings may be validly applied to the very small dissipative scales of high Re number turbulence.

Commercial Laser Doppler Velocimetry (LDV) systems are not adequate to observe low mean velocity flow because of the high frequency shifting of laser light which is typically employed in such equipments. To overcome such a problem a suitable electro-optic frequency shifter has been designed and built up to be used for our experiment. Electro-optic frequency shifters in Laser Doppler anemometry have been considered by different authors (e.g. see Durst and Zaré [11] and references therein]) although their use have been hampered by technological constraints. However, today advances in non-linear optical crystals and devices make it possible to realize very efficient frequency shifter with no mechanical moving parts. The system we have realized allows us to tune the frequency shifting in the range 0-150 kHz with no broadening in the velocity distribution. This tunable frequency shifting may be efficiently matched to the low Doppler frequency (a few kHz) which characterizes low velocity flow.

The paper is organized as follows. Section 2 describes our experimental settings with emphasis on the frequency shifter. Section 3 deals with the estimation of the LDV noise and related variance spectrum. The LDV velocity observations and results are introduced and discussed in section 4. Conclusions are drawn in section 5.

2.Experimental Setting

Our measurements have been made in a water tunnel which has been described in some details in [12]. Basically, the hydraulic part is a closed water tunnel comprised of an horizontal cylindrical pipe 6 m long, whose inner and outer diameters are 0.05 and 0.06 m, respectively, and a water tank which provides water to the horizontal pipe by a direct coupling through a smooth plastic tube whose diameter is 1/5 of the diameter of the water tunnel.

The turbulence we observe (e.g. see [13, 14]) is the result (i): of disturbances at the inlet and (ii) instability of the boundary layer in the inlet region of the pipe. Because of the relatively small value of the Reynolds number we have examined, we expect the first kind of turbulence to dominate.

The LDV system is comprised of an optical part and a data acquisition system. The data acquisition system is a TSI digital burst correlator, model IFA-655, which has been used with the following operating parameters.

- Minimum number of cycles per burst: 8 (this is the maximum allowed by the system);
- Signal-to-noise-ratio mode: high;
- Threshold optimization: 55\%;
- Acquisition mode: Random;
- Data sampling method: TBD on.

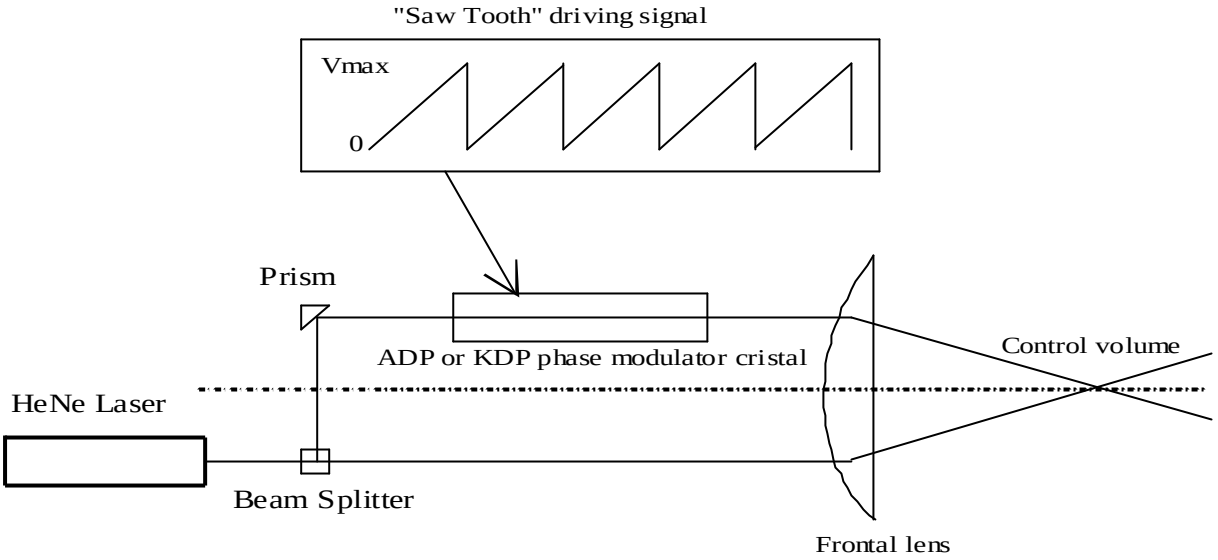

Figure 1: Schematic layout of the new LDV system

The optical part was developed at our laboratory (see the schematic layout of Fig. 1). The test volume is obtained by two incident laser beams generated by a single 20 mW He-Ne Laser. To avoid undesirable refraction from the pipe wall a rectangular cell filled with water was placed around the pipe at the point where measurements were taken. The two beams are obtained by a beam splitter and one of the two is phase modulated through an electro-optic crystal. This is a Pockels cell constituted by four potassium dihydrogen phosphate KDP (KD2PO4) of aperture of 3*3 mm. As well known the Pockels effect is realized when an isotropic transparent substance becomes birefringent if placed in an electric field. Varying the intensity of the electrical field it is possible to vary the birefringent property (i.e. the state of polarization of the incident light). In brief, the birefringence is varied electronically by means of a controlled applied electric field. If the E-field of the incident light is aligned with the crystal optical axis, phase retardation is realized. In this case, if only one beam of the two beams used in the classical LDV set-up, travels into the crystal and the electrical field is linearly varied, the spatial positions of the interference fringes in the control volume is varied.

This variation reaches the maximum when the applied electric field reaches the maximum. At this point no more shift in the fringes position can be realized, but if we suddenly turn off the applied electrical field the fringes are turned back at the original position and a new cycle can be activated. In practice feeding the crystal by an electric field variable whit a "saw tooth" shape, it is possible to generate a continuous shift into the fringe position. The frequency of the realized shift is correlated at the frequency of the "saw tooth" signal. In this way we realized a frequency shift which is tunable in the interval 0-0.15 MHz.

3.Post-processing of the velocity observation

Because of experimental restrictions, only the component of the velocity in the stream wise direction has been measured. Measurements were considered at X/d=100, where X gives the distance from the inlet and d is the inner diameter of the tube. The Reynolds number is 5000. At X/d=100 and for Re=5000 we observe nearly homogenous turbulence (e.g. see [12]). The Reynolds number is defined as usual:

$$\mathrm{Re} = \frac{Ud}{n} \qquad (1)$$

with U the mean flow velocity and n=10^{-6} m^2s^{-1} the kinematic viscosity of water at 20 °C.

Velocity samples were acquired in the so-called *Random* mode and the system was operated in such a way to count up the particles passing through the test volume, so that, in addition to velocity observations, the time between samples was recorded, too. No artificial seeding was employed. The mean data rate was of 1475 Hz.

The nearly continuous series was, then, digitally low pass filtered (re-sampled) in order to have equi-spaced samples. The re-sampling rate, Dt, has been chosen equal to 10 times the inverse of the mean data rate that in our case is 1475 Hz, so that Dt =10/1475 s =0.0068 s. It should be stressed that for the flow we have considered the most

important spectral content develops at small frequency (below 10-30 Hz), so that there is no need to retain a data rate of 1475 Hz which would have only the effect to increase the level of LDV noise.

The low-pass filtering operation consists simply in computing the average value of the velocity during the time interval Dt,

$$V(i\Delta t)=\frac{1}{\Delta t}\sum_{j=1}^{n_i}\Delta t_{ij}u_{ij};\qquad \sum_{j=1}^{n_i}\Delta t_{ij}=\Delta t;\qquad i=1,...,\frac{T}{\Delta t} \tag{2}$$

where u_{ij} indicates the original velocity time series, Dt_{ij} is the time between two consecutive samples u_{ij}, u_{ij+1}; T is the total observational period and, finally, n_i gives the number of velocity samples within each time interval Dt.

3.1 Assessing the magnitude of LDV noise

Especially at low flow velocity, the analysis of the correlation structure on the basis of variance spectra is hampered by the inherent LDV noise component (the so-called ambiguity spectrum, e.g. [15]) which adds a noise floor to the observed power density and tends to level-off the spectrum at high frequency. Nevertheless, this kind of noise is Gaussian, white and has a constant variance (e.g. [15]).

Here we need to distinguish between the re-sampled series $V(iDt)$ which is computed according to Eq. (2) and the original series $u(t_i)$ which is sampled at random times, t_i. The LDV noise may be considered truly random as the level of this last series and its magnitude (variance) may be estimated by exploiting the average properties of the correlation function as we will now show. The noise affects additively the signal so that the observations can be represented according to the following measure model:

$$u(t_i)=u_s(t_i)+w(t_i);\qquad i=1,...,N \tag{3}$$

where u_s is the signal function and w is a noise component with zero mean and finite variance. Let $\tilde{C}(j)$ be the covariance function of the measurements:

$$\tilde{C}(j)=\frac{1}{N-j}\sum_{i=1}^{N-j}\left(u(t_{i+j})-\bar{u}\right)\left(u(t_i)-\bar{u}\right) \tag{4}$$

with $\bar{u}$ the average value of the series $u(t_i)$:

$$\bar{u}=\frac{1}{N}\sum_{i=1}^{N}u(t_i) \tag{5}$$

then

$$\tilde{C}(j)=\begin{cases}s_s^2+s_w^2 & \text{for j=0}\\ \tilde{C}_s(j) & \text{otherwise}\end{cases} \tag{6}$$

provided that the noise component $w(t_i)$ is white.In Eq. (6),$\tilde{C}(j)$ is the covariance function of the signal, σ^2_s is the variance of the signal, σ^2_w is the variance of the error term, and $\sigma^2=\sigma^2_s+\sigma^2_w$ is the variance of the observations. Equation (6) shows that in presence of a white additive error component, the covariance function is biased only at the origin so that an estimation of the LDV noise may be obtained by

$$\hat{s}_w^2=\tilde{C}(0)-\tilde{C}_s(0) \tag{7}$$

provided that we have a suitable way to compute $\tilde{C}_s(0)$. To this end, by keeping in mind that $\tilde{C}_s(j)=\tilde{C}(j)$, for $j>0$, we fit a second-order polynomial to the first N_f data points of the function$\tilde{C}_s(j)$:

$$\tilde{C}_s(j)=a_0+a_1 j+a_2 j^2;\qquad j=1,...,N_f \tag{8}$$

The unknown parameters are obtained by a least-squares fit to the data points. An estimation of $\tilde{C}_s(0)$ is then obtained by extrapolating the function $C_s(j)$ at lag *j=0* through the polynomial (8), that is $C_s(0) = a_0$, and

$$\hat{s}_w^2 = \tilde{C}(0) - a_0 \qquad (9)$$

In our analysis we have $N_f=10$, which means that we consider only data points close the origin where the covariance function is expected to have a parabolic behaviour.

This procedure allows us to get an efficient estimate of the LDV noise variance. However, it should be stressed that the covariance function $\tilde{C}(j)$ cannot be used to analyse the correlation structure of the series $u(t_i)$ itself because of the biases introduced by the fact that the series t_i of times is not even spaced. In addition, $\tilde{C}(j)$ cannot be considered to obtain the variance spectrum through a Fourier transform. This is why we resort to the even sampled series *V(iDt)*.

However, an extra complication now arises because the LDV noise cannot be considered truly random at the level of the series *V(iDt)*. This may happen because a given bin $[t_j, t_{j+1}]$ of width $Dt=t_{j+1}-t_j$ may contains an event, $u(t_i)$ which is started in the previous bin. This event has to be assigned in part to the bin $[t_{j-1}, t_j]$ and in part to the bin $[t_j, t_{j+1}]$. This correlates the noise at the shortest time scales! However, this is not a serious shortcoming. What we do is to generate a surrogate random Gaussian series, $w(t_i)$, with zero mean and variance σ^2_w which perfectly parallel the series $u(t_i)$. This series undergoes the same transformations as those that $u(t_i)$ goes through to obtain the series *V(iDt)*. In the end, we obtain a surrogate random series *W(iDt)* which has exactly the same correlation structure as that of the LDV noise affecting the series *V(iDt)*. The *W(iDt)* series may be used, e.g., to estimate the LDV noise power spectrum to be compared to the power density of the observations.

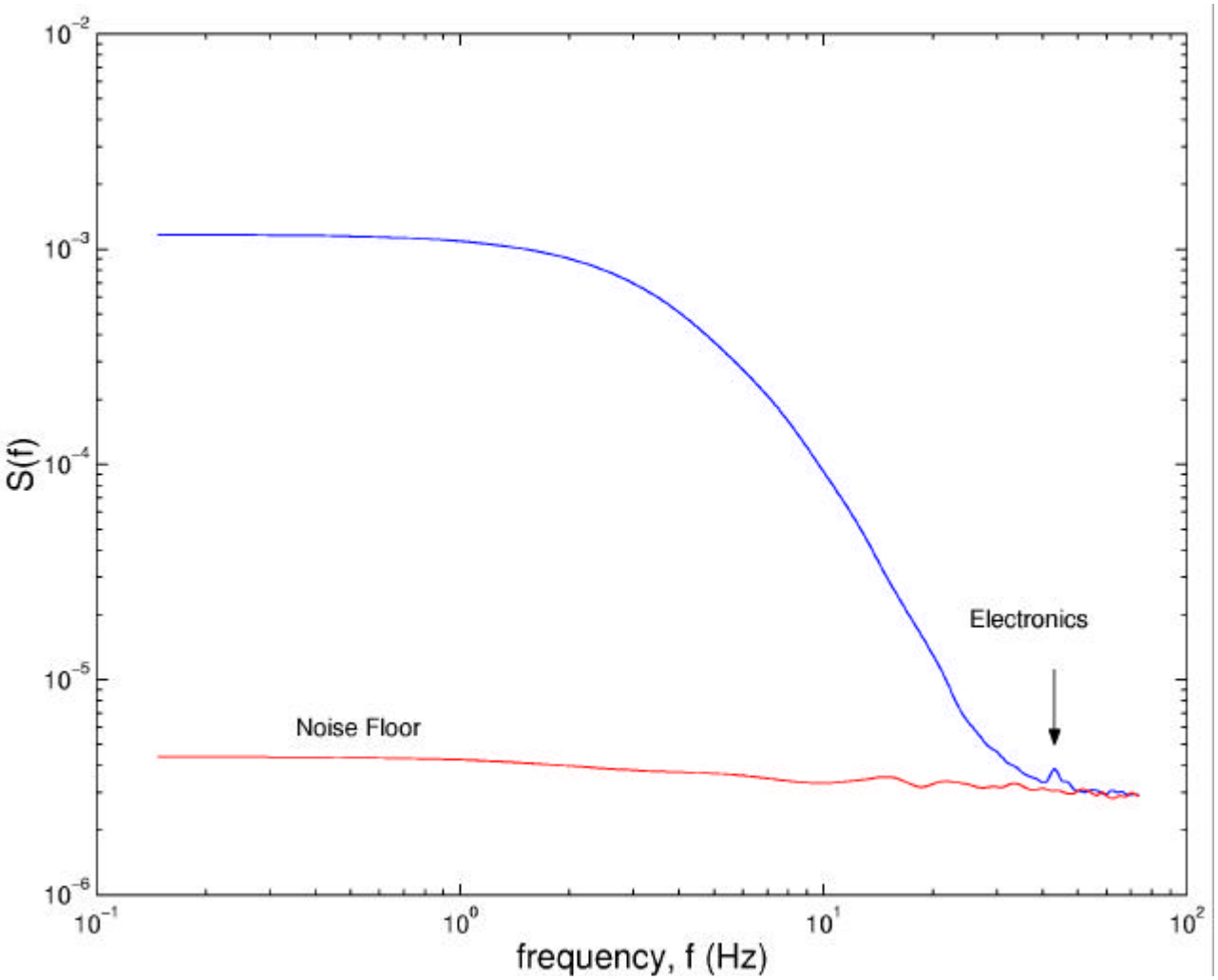

Figure 2: Variance spectrum (m^2/s^2-Hz) against the frequency for the velocity series V(iDt) for Re=5000. The red lines is the power spectrum of the LDV noise affecting the velocity series.

4.Results

The velocity series we have analysed has a mean velocity $\overline{V}=0.13m/s$. The number of data points is $N=2\cdot10^6$ (before re-sampling) and Re=5000. The variance spectrum has been computed by Fourier transforming the covariance function of the re-sampled series *V(iDt)*. The spectrum is shown in Fig. 2 along with the noise spectrum computed via Fourier transform of the covariance function of *W(iDt)*. It is possible to see that at high frequency the spectrum of the observations just converges to the noise floor which leads us to conclude that our methodology to estimate the LDV noise component affecting the series *V(iDt)* is really effective.

Using the methodology described in the previous section, we have estimated for the LDV noise a variance $\hat{s}^2_w=1.59\cdot10^{-6}$ m^2/s^2 which may be compared to the variance of the signal (corrected for the LDV noise) $s^2_V=3.60\ 10^{-5}$ m^2/s^2 which gives a signal-to-noise ratio $s^2_V/s^2_W\approx23$. The same figure is below 1 if we use commercial acoustooptic or mechanical frequency shifting devices (e.g. Bragg cells or rotating diffraction grating).

The result shown in Fig. 2 leads us to conclude that the spectrum, *S(f)* may be modeled as composition of two additive components:

$$S(f)=P(f)+G(f) \tag{10}$$

where *P(f)* is the unknown signal spectrum and *G(f)* is the power density of the LDV noise, this last term being a known quantity.

It should be stressed that in order to check the goodness of some model for *P(f)*, we do not need to subtract *G(f)* from *S(f)*, which could give unrealistic values for frequency such that *P(f)<<G(f)*. A much more suitable strategy is rather to add *G(f)* to the given analytical model *P(f)*, that is to fit *P(f)+G(f)* to the observations *S(f)*. This approach will be taken here.

One model for the spectrum which has been used has a general interpolation formula in the past years (e.g. see [16]) is the Lorentzian-shape model

$$P(f)=\frac{c_0}{1+(f/f_0)^2} \tag{11}$$

with $c_o=P(0)$ and f_o has to be determined from the observations. A best fitting procedure gives $f_o=1.9\ Hz$. However, this function yields only a crude approximation of the observed power density as it is possible to see from Fig. 3.

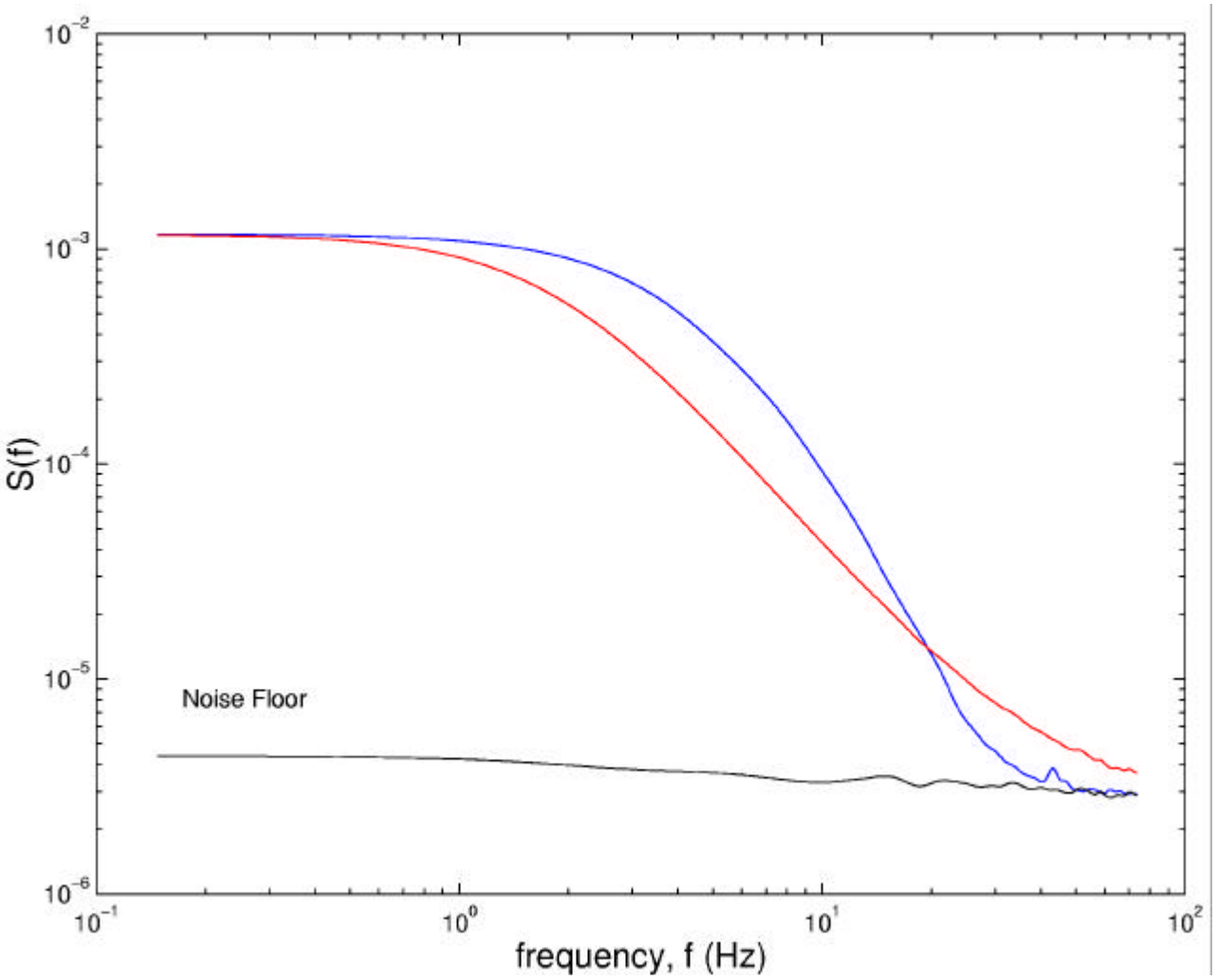

Figure 3: Comparison between the variance spectrum (m^2/s^2-Hz) of the observations (blue line) and the Lorentzian-shape model (red line).}

It appears quite evident from Fig. 3 that the spectrum falls off much rapidly that $1/f^2$ so that to check for the possibility of a fall-off more rapid than $1/f^2$ we consider the model

$$P(f)=\frac{c_0}{1+(f/f_0)^a} \tag{12}$$

where now we allow for an adjustable exponent a. The results are shown in Fig. 4. The fit parameters are f_0=4.7 Hz and a=3.41. The result improves, however a misfit is still evident throughout the frequency range.

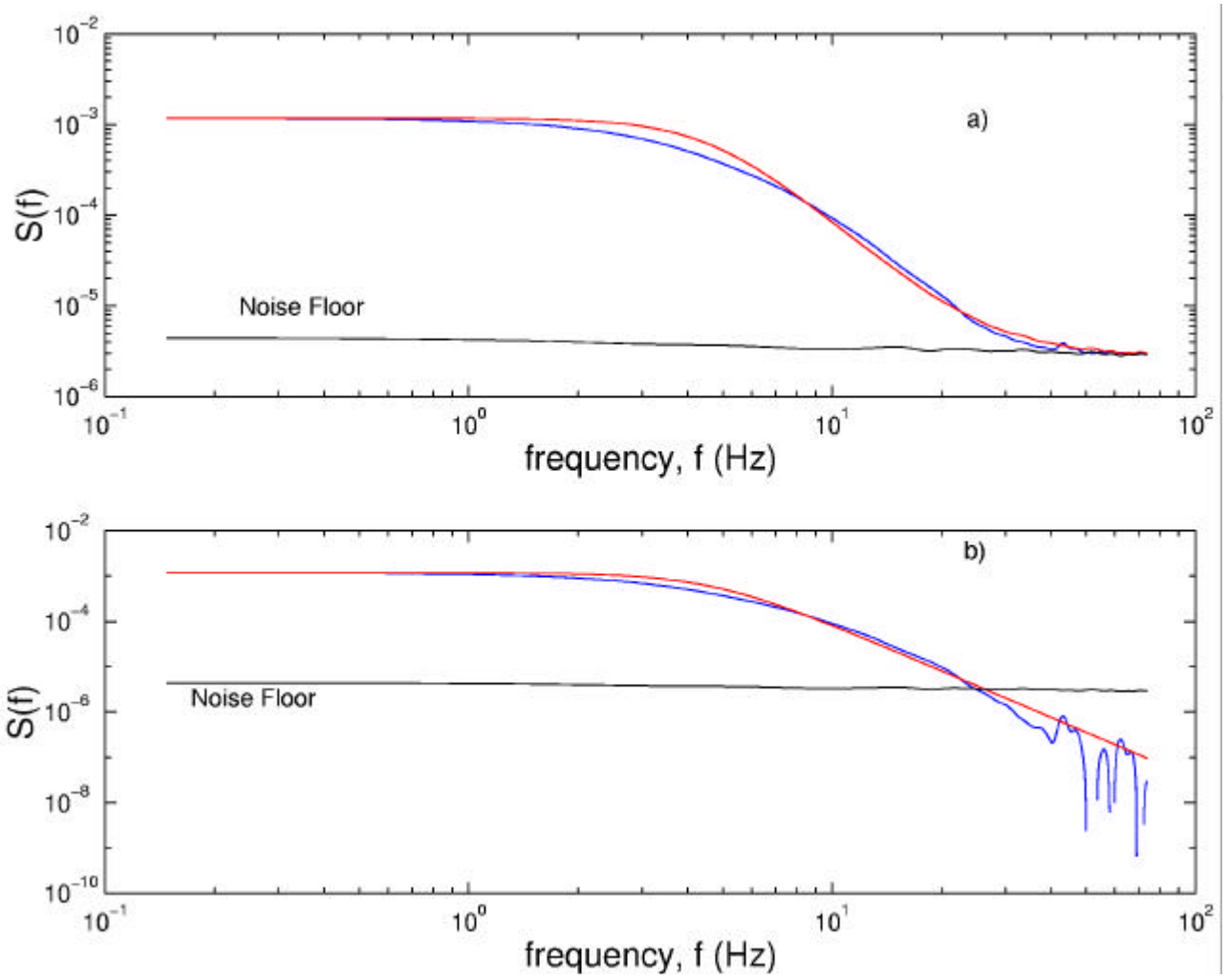

Figure 4: Comparison between the variance spectrum (m^2/s^2-Hz) of the observations (blue line) and the power law (algebraic) model (red line). In b) the noise component G(f) has been subtracted from model and observations.

The failure of the above models could well be the result of the impossibility to fit the spectrum over all the frequency range just one single frequency cut-off. For this reason we combine the above two models to give

$$P(f)=c_0\frac{1}{1+(f/f_1)^2}\frac{1}{1+(f/f_1)^a} \tag{13}$$

which now allows for two cut-off scales. It is possible to see that the fit improves (Fig. 5), however we still have a discrepancy especially at higher frequency. This effect is better seen when correct for the LDV noise, that is when we subtract the component *G(f)* to both the model and observed spectrum. The fit parameters for this case are: f_1=4.31 Hz, f_2=12 Hz and a=2.33.

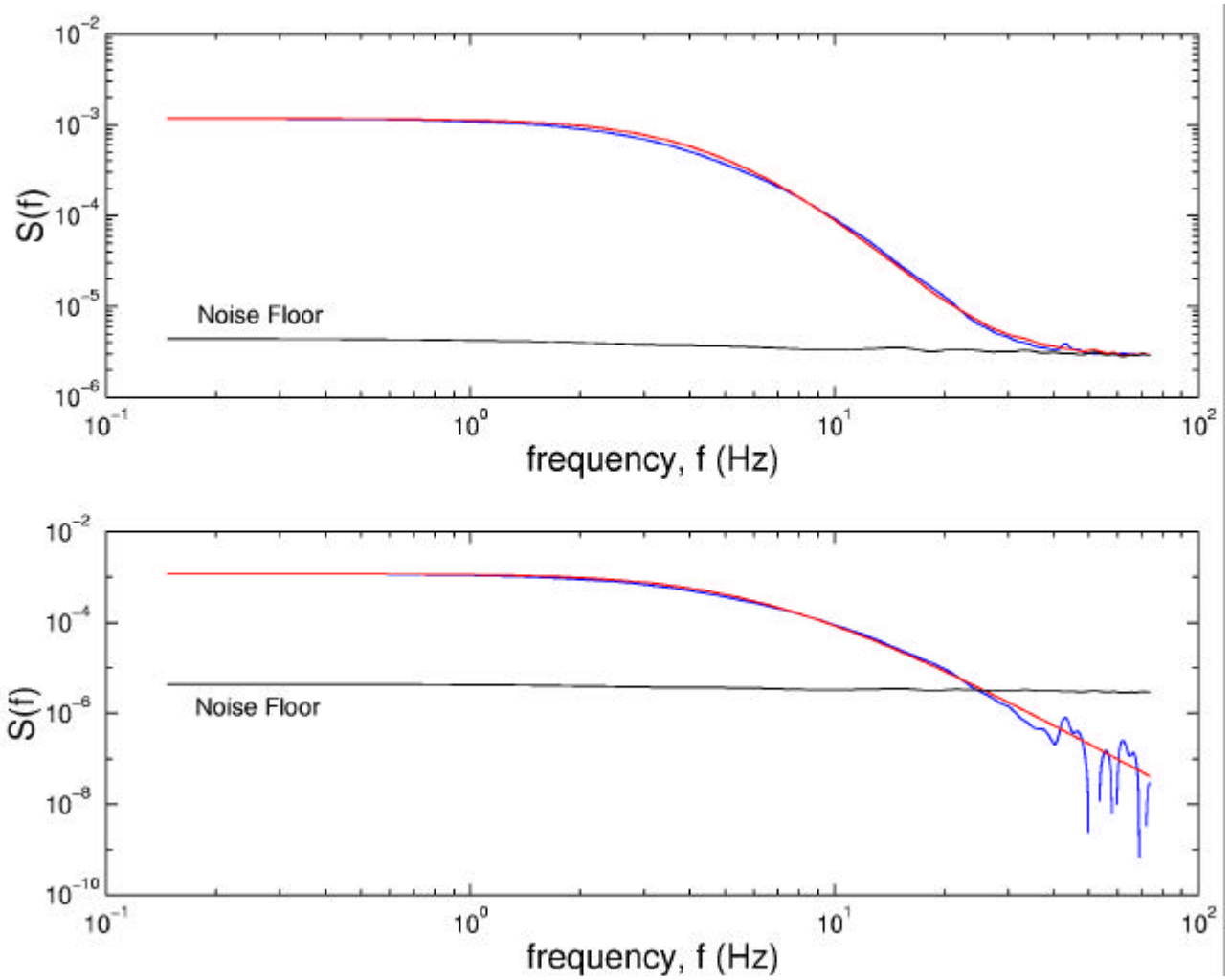

Figure 5: Comparison between the variance spectrum (m^2/s^2-Hz) of the observations (blue line) and the two-scale algebraic model (red line). In b) the noise component G(f) has been subtracted from model and observations.

Finally, we have tested a faster-than-algebraic fall-off of *S(f)* by considering an algebraic pre-factor multiplied by an exponential decay

$$P(f) = c_0 \frac{\exp(-f/f_2)}{1+(f/f_1)^a} \tag{14}$$

The result is shown in Fig. 6. The spectrum is perfectly reproduced at all frequency. This is further evidenced when we remove the *G(f)* component to see below the noise level. The exponential fall-off extends quite well at the highest frequencies.

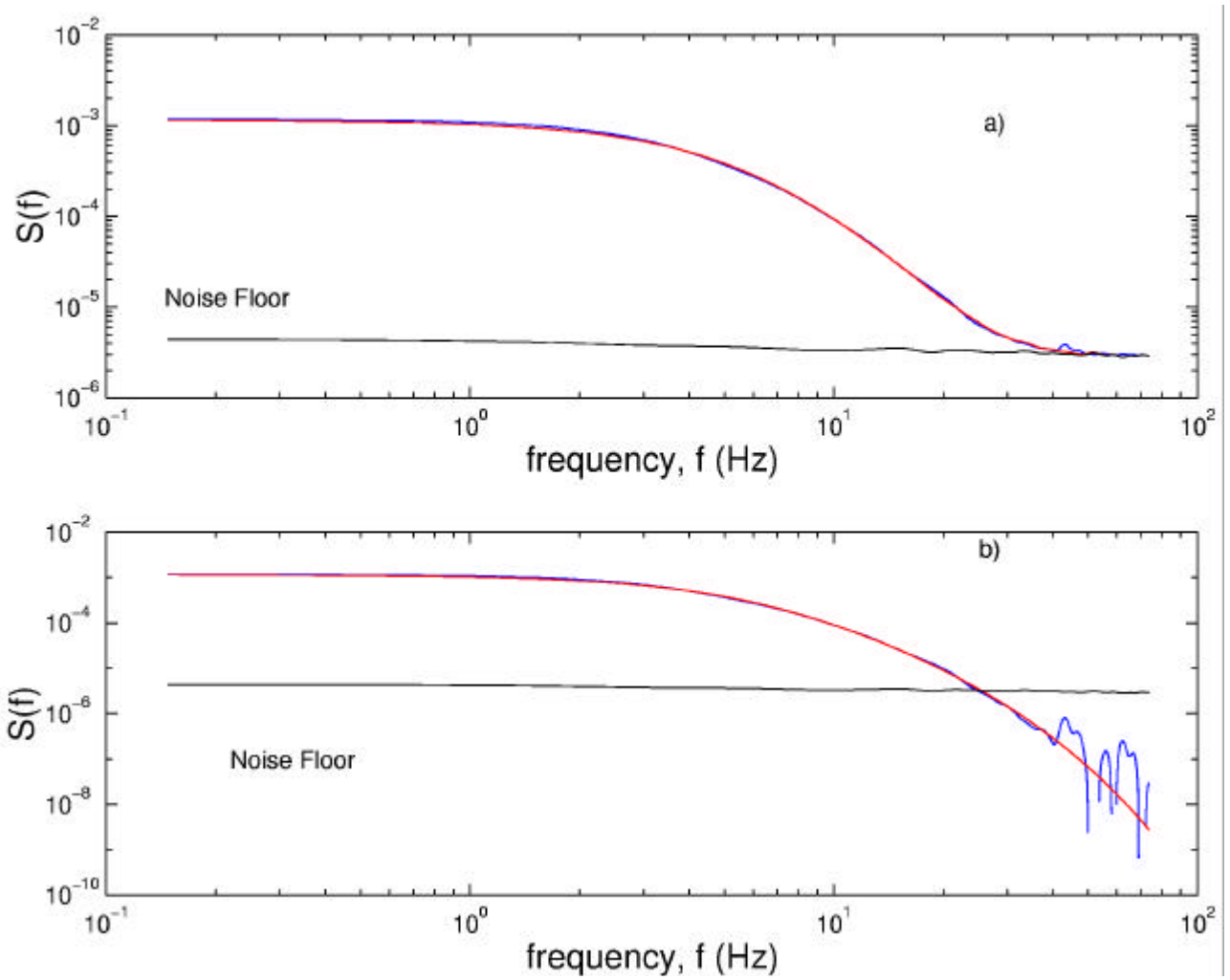

Figure 6: Comparison between the variance spectrum (m^2/s^2-Hz) of the observations (blue line) and the algebraic-exponential two-scale model (red line). In b) the noise component G(f) has been subtracted from model and observations.

It is important to note that the exponent a is quite close to 2 (namely a=2.12), which recovers the well known result that at smaller frequency the Lorentzian-shape behaviour is adequate to describe the variance spectrum [16]. Noteworthy is the presence of two cut-off scales, too. The algebraic cut-off f_1=5.35 Hz dominates the spectrum at smaller frequency, and is followed by a exponential decay with an inverse time constant f_2=10 Hz. We think that this two time constants separate the large scale of the motion from the smaller one. By applying Taylor's frozen turbulence arguments, we have that f_1 corresponds to approximately 2.7 cm, which is almost one half of the pipe diameter, whereas the exponential scale f_2 relates to a spatial scale of about 1.3 cm. It should be stressed that for our experiment the Taylor microscale corresponds to about 35 Hz, so that it seems that the exponential fall-off begins before the deep viscous dissipative range. The position of the Taylor microscale on the frequency axis is shown in Fig. 7 which is the same as Fig. 6 but with a linear scale for the frequency-axis. In Fig. 7 the noise component $G(f)$ has been removed. It is possible to see the Taylor scale is clearly resolved and that the exponential fall-off agrees quite well with the observed spectrum.

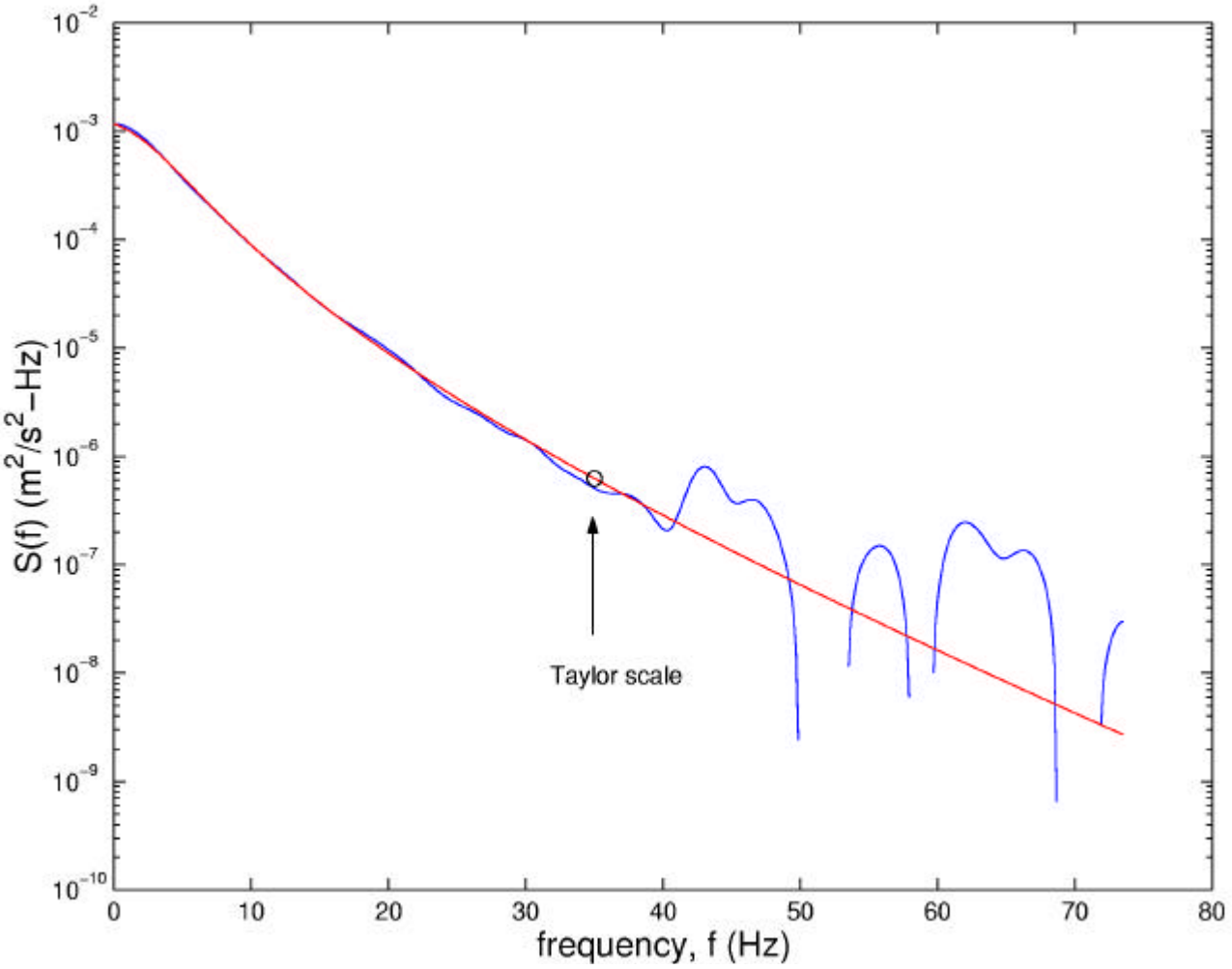

Figure 7: Comparison between the variance spectrum of the observations (blue line) and the algebraic-exponential two-scale model (red line). The noise component G(f) has been subtracted from model and observations. The position of the Taylor microscale is indicated by an arrow.

5.Conclusions

Low Reynolds number pipe flow has been investigated on the basis of LDV measurements. A novel frequency shifting device has been specifically built up for this experiment which allows us to study the flow with a relatively high signal-to-noise ratio. This new measurements have been made it possible to investigate the variance spectrum down to the Taylor microscale, whit a good degree of accuracy. It has been shown that the spectrum decays exponentially in the dissipative range, which, according to Kraichnan [10], is a strong clue for intermittency. This new result still supports that ESS is correct. Finally, it has to be stressed that Kraichnan's arguments [10] are independent of Reynolds number (Re) so that our findings could still apply to the very small dissipation range scales of high Reynolds number turbulence.

Acknowledgments. Work supported by Regione Basilicata (Contract POP N.3) and INFM.

References

[1] G. Paladin and A. Vulpiani, *Phys. Rep*. **156** (1987) 147-225.

[2] B.B. Mandelbrot, *The fractal geometry of nature* (Freeman, New York) 1982.

[3] L.C. Anselmett, Y. Gagne, E.J. Hopfinger, R.A. Antonia, *J. Fluid. Mech*. **140** (1984), 63.

[4] R. Benzi, S. Ciliberto, R. Tripiccione, C. Baudet, F. Massaioli and R. Succi, *Phys. Rev. E* **48** (1993) R29.

[5] R. Benzi, L. Biferale, S. Ciliberto, M. V. Struglia, R. Tripiccione, *Physica D* **96** (1996) 162.

[6] F. Esposito, E. Nino and C. Serio, *Europhys. Lett*. **35** (1996) 653.

[7] R. Camussi and G. Guj, *J. Fluid Mech*. **348** (1997) 177.

[8] C. Serio, *Europhys. Lett*., **42**(6), (1998) 605-609.

[9] P. Kailasnath, K. R. Sreenivasan , and G. Stolovitzky, *Phys. Rev. Lett*. **68** (1992), 2766.

[10] R. H. Kraichnan, *Phys. Fluids* **10**, (1967), 2080-2082.

[11] F. Durst and M. Zaré, *Appl. Opt*. **13**, (1974), 2562-2579.

[12] E. Nino and C. Serio, *European Physical Journal B* **14**, (2000), 191-200.

[13] J. Wygnanski and F. H. Champagne, *J. Fluid. Mech*., **59** (1973) 281-335.

[14] J. Wygnanski and F. H. Champagne, *J. Fluid. Mech*., **69** (1975) 283-304.

[15] F. Durst, A. Melling and J. H. Whitelaw, *Principles and Practice of Laser-Doppler Anemometry*, (Academic Press, London), 1981.

[16] J. O. Hinze, *Turbulence* (McGraw-Hill, New York), 1975.